Chinese Chemical Letters 32 (2021) 3331–3341

Contents lists available at ScienceDirect

Chinese Chemical Letters

journal homepage: www.elsevier.com/locate/cclet

Review

Triphenylamine (TPA) radical cations and related macrocycles

Lijun Mao, Manfei Zhou, Xueliang Shi*, Hai-Bo Yang*

Shanghai Key Laboratory of Green Chemistry and Chemical Processes, School of Chemistry and Molecular Engineering, East China Normal University, Shanghai 200062, China

ARTICLE INFO

Article history:
Received 23 February 2021
Revised 1 May 2021
Accepted 6 May 2021
Available online 14 May 2021

Keywords:
Triphenylamine
Organic radicals
Macrocycles
Redox

ABSTRACT

Triphenylamine (TPA) derivatives and their radical cation counterparts have successfully demonstrated a great potential for applications in a wide range of fields including organic redox catalysis, organic semiconductors, magnetic materials, *etc.*, mainly because of their excellent redox activity. The stability of TPA radical cation has significant effect on the properties of the TPA-based functional materials, especially in relation to their electronic properties. Considering the instability of parent TPA radical cation, many efforts have been devoted to the development of stable TPA radical cations and related materials. Among them, TPA radical cation-based macrocycles have attracted particular attention because their large delocalized structures can stabilize the TPA radicals, thus endow them with outstanding redox behaviors, multiple resonance structures, and wide application in various optoelectronic devices. In this review, we give a brief introduction of organic radicals and the documented stable TPA radicals. Subsequently, a number of TPA radical cation-based macrocycles are comprehensively surveyed. It is expected that this minireview will not only summarize the recent development of TPA radical cations and their macrocycles, but also shed new light on the prospect of the design of more sophisticated radical cation-based architectures and related materials.

1. Introduction

Radicals refer to the atom, molecule, or ion that possess one or more unpaired electrons. Among them, organic radicals are the most common radical species, which play very important roles in the fields of polymer, biological, plasma, and atmospheric chemistry as well as combustion, and many chemical reactions [1-4]. For example, organic radicals featuring special open-shell structures have been widely applied in catalysis, rechargeable batteries, organic semiconductors, magnetic materials, and biologically relevant based materials [5-10]. Organic radicals can be generated through many different methods, for example redox reaction, heat, irradiation, electrolysis and so on [5-10]. One of the most important features of organic radicals is their high instability and transient lifetime, which has severely limited studies of them including their synthesis, characterization, chemical and physical properties and practical applications. The first persistent organic radical, a carbon-centered triphenylmethyl radical **1** (Fig. 1a), was first reported by Gomberg in 1900 [11]. However, triphenylmethyl radical **1** itself is not enough stable and readily undergoes dimerization especially in the solid state (Fig. 1a). Since then, a great deal of effort has been devoted to the molecular-level understanding of the stability, structural and electronic properties of organic radicals, which greatly promoted the development of modern organic radical chemistry [5-10]. Generally, organic radicals can be either thermodynamically stabilized or kinetically stabilized and their stabilities are affected by many factors such as molecular conjugation, hybridization, hyperconjugation, captodative effects, steric effects and so on. Based on the understanding of these stabilization factors together with the advanced organic synthesis and modern characterization techniques, various carbon-centered and related stable radicals have been successfully developed by chemists over the last century [5-16]. The representative examples are tris(2,4,6-trichlorophenyl)-methyl radical **3** [17], Koelsch radical **4** [18], 2,2′:6′,2″:6″,6-trioxytriphenylamine **5** [19], and phenalenyl radical **6** [20] (Fig. 1b), which exhibit robust stability mainly due to the thermodynamical or kinetical stabilization considerations in their molecular design. In addition to the carbon-centered radicals, heteroatom-centered radicals (Fig. 1c), including neutral radical, radical cation, and radical anion, for example, nitroxide radical 2,2,6,6-tetramethylpiperidine 1-oxyl **7** [21], thianthrene

* Corresponding authors.
E-mail addresses: xlshi@chem.ecnu.edu.cn (X. Shi), hbyang@chem.ecnu.edu.cn (H.-B. Yang).

https://doi.org/10.1016/j.cclet.2021.05.004
1001-8417/

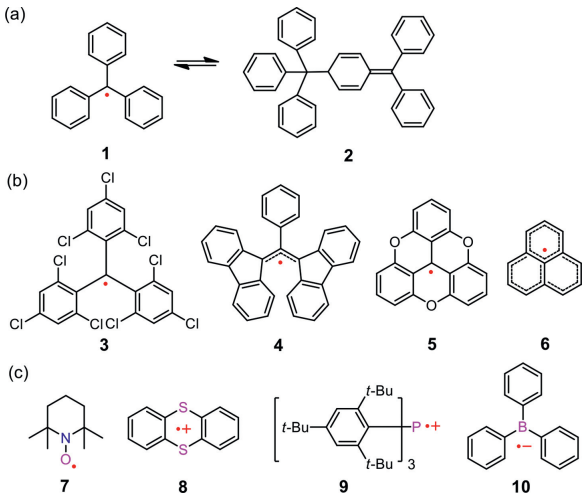

Fig. 1. (a) Chemical structure of triphenylmethyl radical **1** with its dimmer product **2**. (b) Some stable carbon-centered radicals **3**–**6**. (c) Some stable heteroatom-centered radicals **7**–**10**.

radical cation **8** [22], triarylphosphine radical cation **9** [23] and boryl radical anion **10** [24], have also been extensively investigated because of their ease of synthesis and relatively enhanced stability.

Among various reported stable organic radicals, triphenylamine (TPA) radical cations as a unique organic radical species have successfully demonstrated a great potential for applications in a wide range of fields including organic redox catalysis, organic semiconductors, magnetic materials, *etc.*, mainly because of their excellent redox activity [25-27]. Triphenylamine possesses low ionization potential due to the conjugation of the nitrogen electron lone pair with the phenyl rings and thus is prone to generating TPA radical cation under the condition of oxidation, irradiation, or direct electrolysis. The stability of TPA radical cation has significant effect on the properties of the TPA-based functional materials, especially in relation to their electronic properties. The structure of TPA radical cation **11** has ten resonance structures (Fig. 2a) and the spin density is mainly distributed on the nitrogen and the *ortho* and *para* carbon atoms (Fig. 2b), which is much alike that of the reported triphenylmethyl radical (Fig. 1a). Thus, TPA radical cation could be regarded as the isoelectronic structure of the triphenylmethyl radical. Similar to triphenylmethyl radical, parent TPA radical cations are highly reactive and could undergo dimerization and polymerization, thus could not isolate in pure crystalline form [25-27]. In consideration of the instability of parent TPA radical cations, extensive efforts have been devoted to developing stable TPA radical cations and their derivatives (Fig. 2c). The prevalent strategies to design and synthesize the stable TPA radical cations are based on the following considerations: 1) when parent TPA is introduced by some substituents, especially at the *para*-position, the stability of the corresponding radical cation could be significant enhanced through preventing the dimerization reaction of TPA [25-27]; 2) when the parent propeller-shaped TPA is planarized with some bridge atoms like C, N, O, S and so on, the resultant TPA radical cation is usually considerably stable because the N-centered radical cation is delocalized over the planarized π-system as well as the heteroatoms [28-30]; 3) weakly coordinating anions (WCAs) such as SbF_6^-, $SbCl_6^-$, $[Al(ORMe)_4]^-$, have demonstrated to be very conducive to stabilize and crystallize the TPA radical because most of the *p*-block cations are very reactive with high electrophilicity, oxidizing ability and coordination ability which could be dampened kinetically by the use of suitable WCAs [31-33].

Among the various TPA radicals, TPA radical cation-based macrocycles have also attracted particular attention due to the

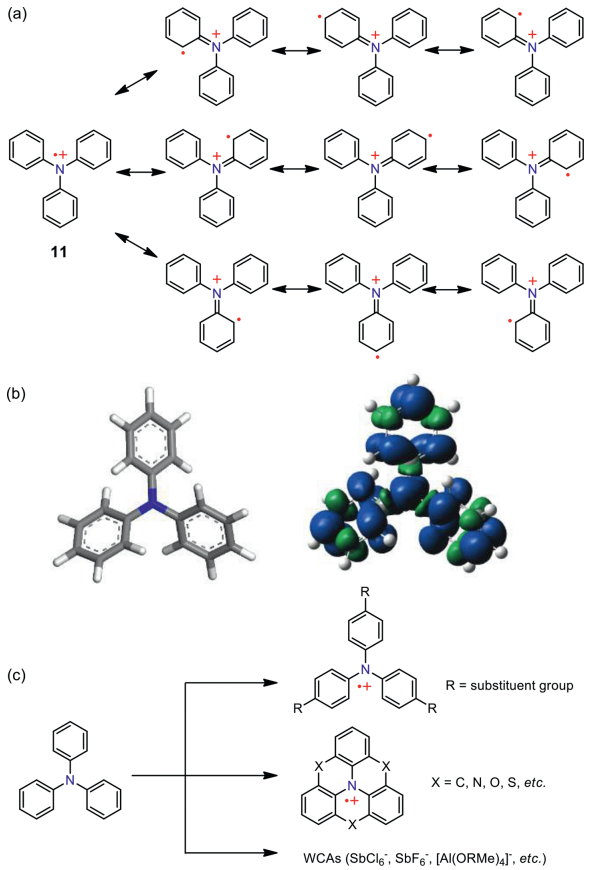

Fig. 2. (a) Ten resonance structures of TPA radical cation **11**. (b) DFT calculated structure of TPA radical **11** (left) and its spin density map at the UB3LYP/6–31G* level of theory. (c) The strategy to synthesize TPA radical cations.

convenience of synthesizing macrocycles, their largely delocalized structures, multiple resonance structures, and potential applications in various optoelectronic devices [34]. First, the ideal geometry of TPA unit with approximate 120° angle makes it ideally suited to construct various TPA-based macrocycles. Second, TPA-based macrocycles possessing large π-conjugated delocalized structures can significantly disperse the spin density, which is conducive to improving the stability of TPA radical macrocycles. In addition, there are many outstanding electronic properties about TPA radical macrocycles, such as tunable geometries and π-conjugation, excellent redox behavior and multiple resonance structures, which endow them with widely potential applications. For example, a plenty of reported macrocycles decorated with triphenylamine moiety [35-43] have been widely used in the field of host-guest interaction, sensing, bioimaging, and optoelectronic materials.

In this review, the design principle, preparation method, as well as the application of TPA-based radicals are briefly described. Subsequently, this review summarizes the recent development of TPA radical cation-based macrocycles, mainly focuses on their synthesis, redox properties, and radical characters. This review is not intended to be comprehensive, and a number of TPA radical cation-based macrocycles are particularly surveyed. Notably, though a number of TPA-based macrocycles have been reported, the studies of their radical cation counterparts, especially their single crystals and practical application, still remain largely unexplored, thus a big exploration research space exists in this topic. The purpose of this review is to facilitate students and researchers understanding the properties of TPA radical cations and related macrocycles, and potentially to stimulate the development of more sophisticated radical cation-based architectures and related functional materials.

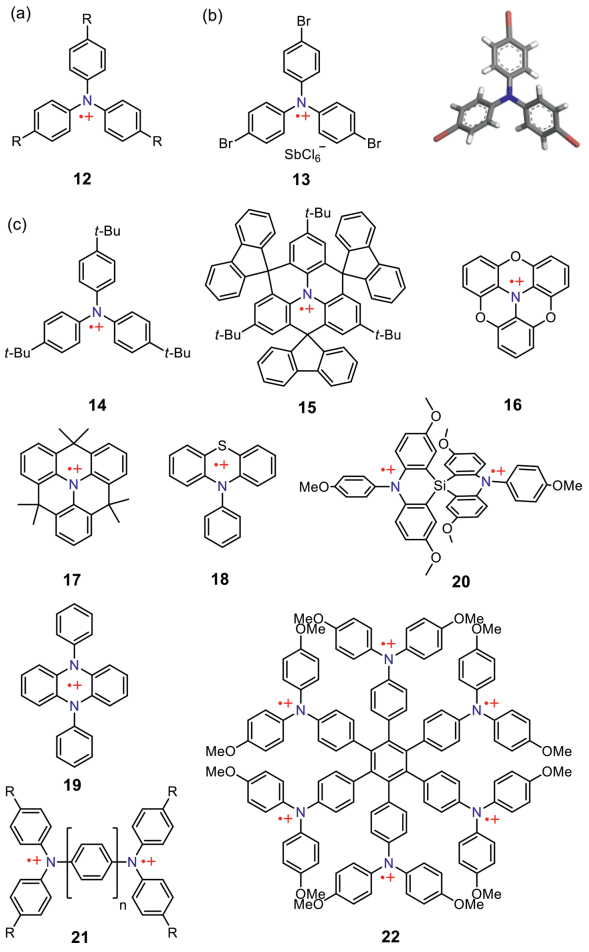

Fig. 3. (a) The first TPA radical cation **12**. (b) Chemical and single crystal structure of magic blue **13**. (c) Some representative stable TPA radicals **14**–**22**.

2. Stable TPA radical cations and related materials

Generally, TPA radical cations without *para* substituents are very reactive because of the large spin densities of the *para* positions, thus facilitating the intermolecular dimerization. The first documented *para*-substituted triphenylamine cation radicals **12** (Fig. 3a) were reported before 100 years ago [44], whose three *para*-positions were protected by bromine or methyl. The relatively enhanced stability of **12** than that of parent TPA **11** is largely attributed to the protection of the *para*-position which prevents the potential intermolecular dimerization. Indeed, tris(4-bromophenyl)ammoniumyl hexachloroantimonate **13**, also known as "magic blue", is a stable radical cation and has already been commercialized as a widely used one-electron oxidant. The *para* bromo–substituted TPA together with the weakly coordinating anion of hexachloroantimonate ($SbCl_6^-$) are crucial for the stabilization of **13**. However, "magic blue" usually undergoes slowly dimerization in the solid state upon storage to form so called 'blues brothers', which might because of the small steric hindrance of Br atom and the weak Br-C bond dissociation energy [45]. To avoid the intermolecular dimerization reaction and further promote their stability, some *para*–*tert*–butyl substituted TPA radical cations such as **14** [46] and **15** [28] have been successfully developed, which show better stability than that of magic blue. Notably, **15** seems to be more stable than **14**, because the parent propeller-shaped TPA is fully planarized in **15** and thus the *N*-centered radical cation is delocalized over the planarized π-system. Though most of the reported stable TPA radical cations are *para*-substituted ones, the non-*para*-substituted example of the oxygen-bridged triphenylamine radical cation **16** displays good stability as well [29]. The unexpected stability of **16** is believed to correlate with its good molecular planarization which facilitates not only the spin delocalization over the whole π-system but also the partial spin delocalization on oxygen atoms. Similarly, the methylene-bridged triphenylamine **17** also shows moderate stability and can be isolated in single crystal form. Interestingly, **17** could further be oxidized in the presence of trace amounts of silver salt to form a stable bis(triarylamine) dication [30]. Some other triphenylamine derivatives **18** [47] and **19** [48], such as phenothiazine and phenazine containing heteroatoms of S and N usually displayed extraordinary stability because the spin could be largely delocalized on the heteroatoms. In addition to the monoradical cation, some TPA-based diradical dication and polyradical polycation have also been successfully prepared. For example, the spirofused radical cation **20** was reported to have a triplet ground state and display interesting ferromagnetic interaction [49]. In contrast, bis(triarylamine) dications **21** showed a characteristic resonance structure between an open-shell diradical and a closed-shell quinonoid form which could further excite to triplet state [25]. The hexaarylbenzene functionalized with six triphenylamine units of **22** could undergo intriguing electron transfer process because of the excellent multiple redox behavior of TPA core [50]. Consequently, **22** was recently employed as hole transporting materials for efficient perovskite solar cells [51].

Triphenylamine and its derivatives as a kind of multifunctional materials have also been attracting considerable attention from both the academia and the industry due to their unique radical properties. The parent triphenylamine unit can be chemically modified with different functional groups which can result in several of multifunctional materials displaying potential application prospect in the field of organic magnet, organic conductor, energy storage, organic solar cells, electroluminescence, and chemical sensors. For example, the inherent stability of TPA radical cation makes it a good stable spin source for the design of high-spin compounds. A high-spin polymer **23** based on triphenylamine radical cations was reported to display a pure quintet state with interesting intracyclophane (J/k = 89 K) and intercyclophane (J/k = 17 K) exchange coupling [52]. Triphenylamine radical cation has also aroused some attention in the field of supramolecular self-assembly. Giuseppone and coworkers made interesting discovery that the light-induced formation of triphenylamine cationic radicals **24** could facilitate the molecular stacking and the subsequently hierarchical self-assembly of nanowires which display metallic conduction properties [53]. The excellent redox behavior of triphenylamine derivatives also makes them good candidate in the field of lithium battery. Polytriphenylamine derivative **25** was successfully employed as a promising cathode material for organic free radical batteries due to its stable chemical structure and high free radical density [54]. Besides, triphenylamine derivatives as a class of versatile redox-active materials have attracted particular attention in relation to their promising hole transport properties. One of the most important hole transport materials (HTMs) based on TPA is the commercialized Spiro-OMeTAD **26** which is widely used for dye sensitized solar cells (DSSCs) and perovskite solar cells (PSCs) [55]. The intrinsic dimerization reaction of TPA also renders it as unique pendant redox-active moieties in polymers to constructed crosslinked polymer films **27** [56]. Moreover, TPA-based polymers have demonstrated great potential as excellent photonic and electroactive materials due to their outstanding physical, photochemical and electrochemical properties. Since there are plenty of reports about the interesting properties and applications of TPA-based conjugated materials, which are also highlighted in many reviews, thus will not be discussed more in this review (Fig. 4).

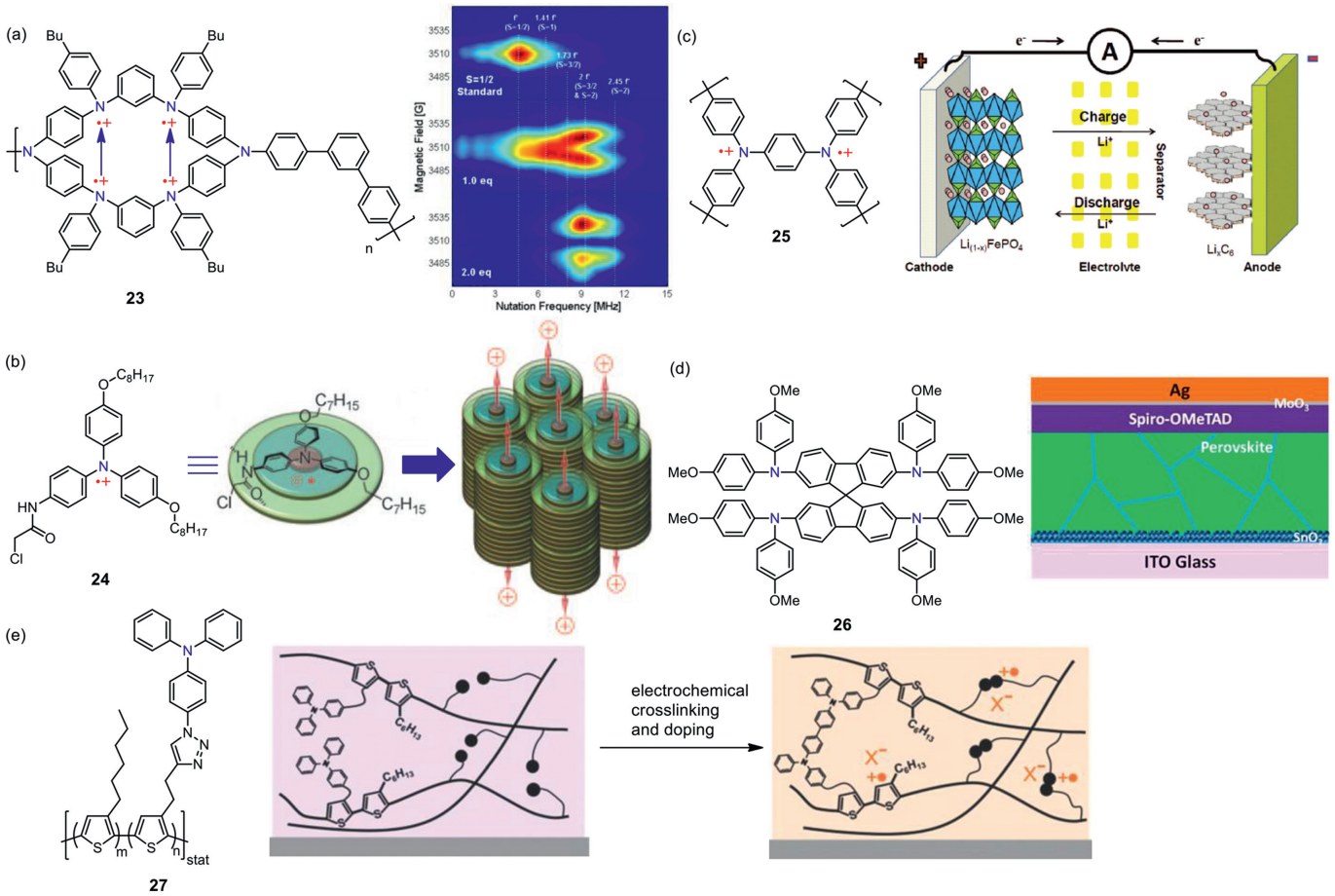

Fig. 4. The TPA radical-based materials. (a) Chemical structure of polymer **23** and its 2D field swept pulsed-EPR nutation spectra. Reproduced with permission [52]. Copyright 2017, American Chemical Society. (b) Chemical structure of **24** and its hierarchical self-assembly processes. Reproduced with permission [53]. Copyright 2010, John Wiley and Sons. (c) Chemical structure of **25** and cathode material in lithium ion batteries. (d) Chemical structure of **26** and device structure of perovskite solar cells. Reproduced with permission [55]. Copyright 2020, American Chemical Society. (e) Chemical structure of **27** and its electrochemical crosslinking and doping process. Reproduced with permission [56]. Copyright 2020, Royal Society of Chemistry.

3. TPA radical-based macrocycle

Among the various well-developed macrocycles [57-87], radical-based macrocycles have gained great attention for their interesting host-guest chemistry, unique electronic structure, and potential application in optoelectronic devices. For example, Stoddart and co-workers reported discrete open-shell tris(bipyridinium radical cationic) inclusion complexes based on cyclobis(paraquat-*p*-1,4-dimethoxyphenylene)tetrakis(hexafluorophosphate) radical cation macrocycle and methyl viologen radical cation [88]. Wu and co-workers recently reported a series of fully conjugated macrocyclic polyradicaloids which display very intriguing radical character and global aromaticity [89-91]. Rai and co-workers reported new donor-acceptor conjugated macrocycles with polyradical character and global aromaticity, which is suitable for numerous optoelectronic applications [92]. Among the plentiful radical macrocycles, TPA radical cation-based macrocycles exhibit outstanding electronic properties, such as tunable geometries and π-conjugation, excellent redox behavior and multiple resonance structures and so on.

TPA-based spin clusters and polyradicals had been well studied, which can be used to prepare and test new electron spin-coupling modes. However, it is problematic to control the conformational relationship between spin-bearing functions. One effective method is to limit conformational freedom in cyclic system. Blackstock et al. synthesized neutral TPA macrocycles **28** and **29** (Fig. 5) with the ability to generate conformationally rigid polyradical cations in one-step Ullmann coupling [93]. The cyclic voltammogram (CV) of macrocycles **28** and **29** showed four and one reversible waves, respectively, indicating that macrocycles **28** and **29** can be oxidized to their corresponding radical species. Macrocycle

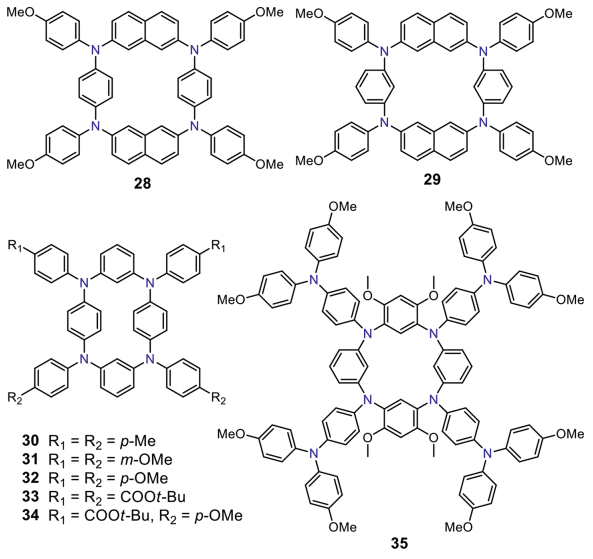

Fig. 5. Chemical structures of macrocycles **28**–**35**.

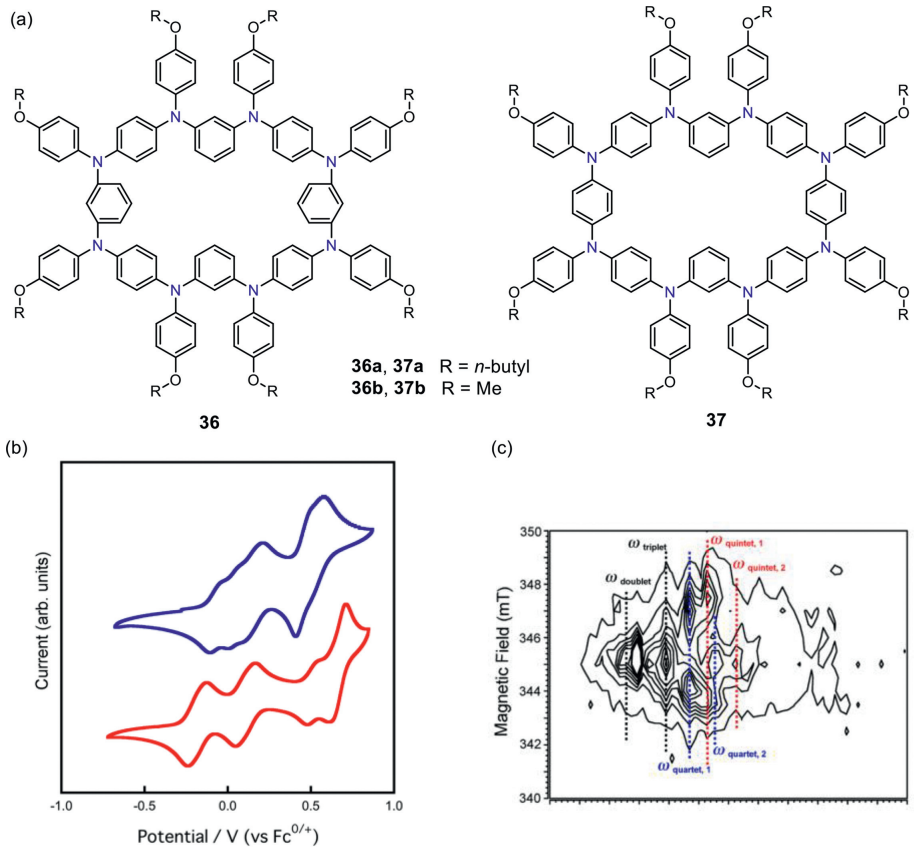

Fig. 6. (a) Chemical structures of macrocycles **36** and **37**. (b) CV of macrocycle **36a** (blue) and **37a** (red). (c) ESTN of macrocycle **36a**$^{4+}$. Reproduced with permission [96]. Copyright 2013, American Chemical Society.

28^{2+} was a thermally populated, low-lying triplet dication from EPR and NMR spectra, while **29** underwent multielectron oxidation. Subsequently, Hartwig *et al.* synthesized high spin ground states geometrically well-defined diradical cation from macrocycles **30**–**34** (Fig. 5) which were obtained in a one-step palladium-catalyzed Ullmann coupling [94]. Diradical macrocycles generated by oxidation reaction were stable at room temperature, which were demonstrated to be in high spin ground states through CV, UV–vis, and EPR spectroscopy measurements. The distance between the two radical sites in **30**$^{2+}$ and **32**$^{2+}$ was approximated by analysis of EPR zero-field splitting parameters. Though TPA radical macrocycles were synthesized through oxidation reaction, macrocycles **28**–**34** cannot generate higher order polycation states on account of the stronger Coulombic repulsion interaction.

Organic molecules with high-spin ground states (total spin quantum number $S \geq 1$) are of fundamental interest to chemistry and physics, because they provide insight into how molecular structure affects the interaction of electrons and leads to macroscopic properties (*e.g.*, magnetism). For purpose of overcoming strong Coulombic repulsive interactions and obtaining higher order polycation state macrocycles, Ito *et al.* introduced 4-aminophenyl group to the TPA macrocycle **35** skeleton (Fig. 5) [95]. CV and UV–vis-NIR spectra of macrocycle **35** indicated the formation of higher oxidation states **35**$^{4+}$ and **35**$^{8+}$. However, **35**$^{4+}$ and **35**$^{8+}$ were unstable in CH_2Cl_2 at room temperature. The spin states of stable macrocycles **35**$^{2+}$ and **35**$^{4+}$ at low temperature were unequivocally determined to be spin-triplet and spin-quintet, respectively, on the basis of the pulsed-EPR studies. This research demonstrated delocalization of spin density can overcome strong Coulombic repulsive interactions which can generate radical macrocycles with higher oxidation states.

What is more, Ito *et al.* proved that insertion of *p*-phenylendiamine (PD) units into macrocycle backbones can also lead to alleviation of the Coulombic penalty. Ring-size extended octaaza-macrocycles **36a** and **37a** (Fig. 6a) were synthesized through Buchwald-Hartwig reactions [96]. DFT calculations on the model compounds **36b** and **37b** indicated that the expansion of macrocycle caused the facile conformational changes, which was categorized into non-disjoint or coextensive molecules, and thus can generate high-spin states. CV of **36a** and **37a** roughly showed four reversible oxidation peaks (Fig. 6b) in CH_2Cl_2, which meant **36a** and **37a** exhibited multi-redox activity. UV–vis-NIR absorption spectral of **36a** and **37a** were conducted *in situ* to demonstrate that PD moieties in **36a** could be converted from the semiquinoidal structure to the quinoidal structure with increasing oxidation number, while higher oxidation states of **37a** did not show definite quinoidal deformation of PD moieties. In addition, from the pulsed EPR spectrum (Fig. 6c), the **36a**$^{2+}$ and **36a**$^{4+}$ showed high-spin states which would transfer to their low-spin states at low temperatures. In contrast, **37a**$^{2+}$ generated almost pure spin-triplet state. This research not only successfully demonstrated that overcoming strong Coulombic repulsive interactions can generate higher oxidation state macrocycles but also revealed that extended macrocycle did not affect the high-spin correlation, which was very important to provide insight into how molecular structure affects the interaction of electrons and leads to macroscopic properties (*e.g.*, magnetism).

Although radical polymers have been studied for a long time, spins of these radical polymers are mainly uncoupled with $S = 1/2$ due to their coil-like conformation that does not favor the ordered spin alignment, leading to negligible spin-spin (radical-radical) coupling. In order to obtain system with coupled spins,

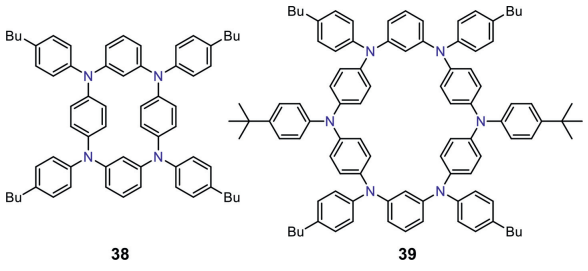

Fig. 7. (a) Chemical structures of macrocycles **38** and **39**.

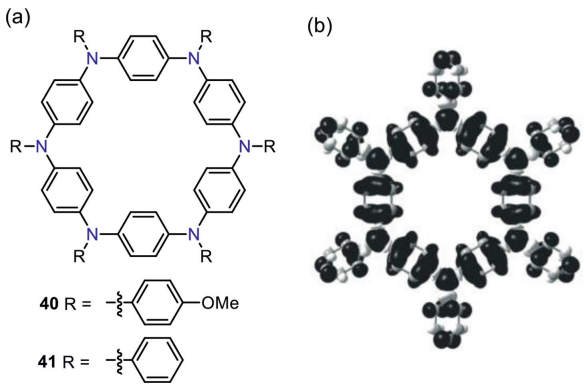

Fig. 8. (a) Chemical structures of macrocycles **40** and **41**. (b) Spin density distribution of macrocycle **41**. Reproduced with permission [98]. Copyright 2010, John Wiley and Sons.

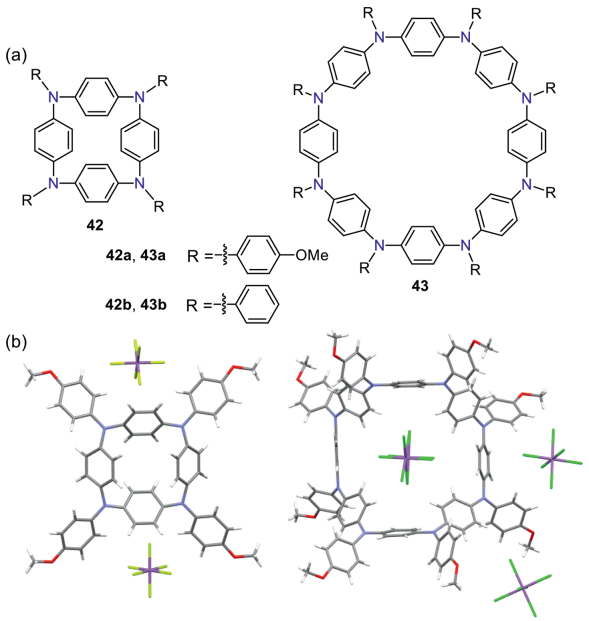

Fig. 9. (a) Chemical structures of macrocycles **42** and **43**. (b) Single crystals of macrocycles $\mathbf{42}^{2+}2SbF_6^-$ (left), and $\mathbf{43a}^{6+}6SbF_6^-$ (right).

Kulszewicz-Bajer *et al.* synthesized tetraazacyclophane **38** and hexaazacyclophane **39** (Fig. 7) at medium concentration *via* a one-step palladium catalyzed amination reaction [97]. The new absorption band in UV–vis-NIR spectra indicated that macrocycles **38** and **39** can be oxidized to different radical states. Spins of both diradical macrocycles can interact ferromagnetically and create almost pure triplet state, which was absent in most radical polymers. This research indicated that TPA macrocycles can be potentially applied to prepare magnetic materials in the future.

Nitrogen-bridged radical metacyclophanes have been investigated due to their novel structure-property and potential application to act as organic magnetic materials. Ito and Tanaka *et al.* reported the preparation of macrocycle **40** (Fig. 8a) through stepwise synthesis for the first time [98]. The radical macrocycle can be generated through oxidation reaction with tris(4-bromophenyl)aminium hexachloroantimonate at 195 K. The EPR spectrum of the resultant macrocycle radical cation exhibited multiplet hyperfine structure attributed to the 6 nitrogen and 24 hydrogen nuclei, indicating the largely delocalized spin distribution within the framework of **40** (Fig. 8b). In addition, macrocycle **40** with high electron donating ability could form charge transfer complex with 7,7,8,8-tetracyano-*p*-quino-dimethane (TCNQ), and the signal of the resulted charge transfer complex can be observed in both Vis/NIR and FT-IR spectra. Subsequently, Yang, Kuo, and Su *et al.* synthesized macrocycle **41** (Fig. 8a) without anisyl at the *para*-position [99], whose conformation was calculated to be non-coplanar based on B3LYP/6–31G** level with the GAUSSIAN 09 program. CV of macrocycle **41** showed two different and reversible oxidation waves, which indicated that **41** can be oxidized to stable radical macrocycle species. Interestingly, **41** exhibited different oxidation waves upon the change of electrolyte due to the host-guest interactions between the radical cation macrocycle and anions from the electrolyte. The new absorption band in UV–vis-NIR spectra indicated that macrocycle **41** can be oxidized to different states. What is more, macrocycle **41** exhibited a blue light emission at 474 nm. This work indicated that this kind of TPA radical macrocycles may have the potential to be used in hole-transporting layer of light-emitting device.

Notably, although a few of such nitrogen-bridged metacyclophanes had been studied, there was no single crystal of their TPA radical counterparts to be published until 2017. Sakamaki, Ito, and Seki *et al.* successfully obtained single crystal of radical macrocycles generated from macrocycle **42** and **43** (Fig. 9a) [100]. Single crystal of neutral macrocycle **42a** indicated that its structure was highly symmetric. Electrochemical measurements of **42a** and **43a** showed that they can be reversibly oxidized up to diradical and octaradical species, respectively. At the same time, absorption spectra of **42a** and **43a** likewise demonstrated the two macrocycles can be oxidized to different radical cations. The EPR measurements of $\mathbf{42a}^+$ and $\mathbf{43a}^+$ demonstrated the full delocalization of spin density over the whole macrocycles on the EPR time scale. Then, the dication of $\mathbf{42a}^{2+}2SbF_6^-$ and the supercharged hexacation of $\mathbf{43a}^{6+}6SbF_6^-$ were isolated as stable salts, whose structures were confirmed by X-ray crystallography. Interestingly, $\mathbf{43a}^{6+}6SbF_6^-$ encapsulated one $SbCl_6^-$ anion in its cavity (Fig. 9b). This is the first example to obtain single crystal of TPA radical macrocycle.

The singlet-triplet energy gaps ($\Delta E_{S\text{-}T} = 2J$) or exchange coupling strength (J) are the degree of interaction between the unpaired electron and the perturbing nuclei, which are the important property of radicals. Researches in this area focused more on the synthesis of TPA radical macrocycles and their radical properties, while the singlet-triplet energy gaps or exchange coupling strength of diradical macrocycle associated with their magnetic properties have rarely been studied. Ito *et al.* synthesized two macrocycles **44** and **45** (Fig. 10a) [101], which can generate radical species $\mathbf{44}^{2+}2SbF_6^-$ and $\mathbf{45}^{2+}2SbF_6^-$. The bond length alternation (BLA) analysis of $\mathbf{44}^{2+}$ and $\mathbf{45}^{2+}$ disclosed that $\mathbf{44}^{2+}$ formed a quinoidal structure, while $\mathbf{45}^{2+}$ formed a structural deformation of the *m*-phenylenediamine moieties, which indicated the spin density of $\mathbf{44}^{2+}$ and $\mathbf{45}^{2+}$ were delocalized and localized, respectively. The $\Delta E_{S\text{-}T}$ of $\mathbf{44}^{2+}2SbF_6^-$ and $\mathbf{45}^{2+}2SbF_6^-$ were successfully determined to be 0.3 kcal/mol and −1.0 kcal/mol, respectively by means of the SQUID measurements (Fig. 10b), indicating the triplet ground state for $\mathbf{44}^{2+}2SbF_6^-$ while the singlet ground state for

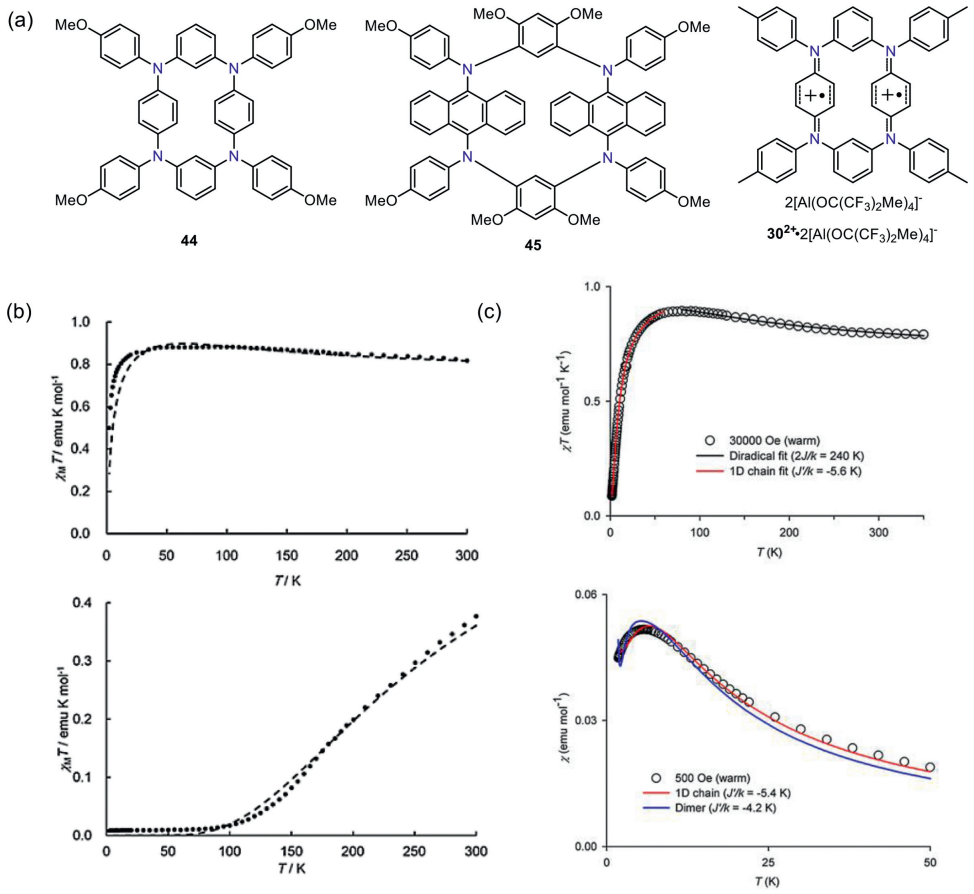

Fig. 10. (a) Chemical structures of macrocycles **44, 45**, and $\mathbf{30}^{2+\cdot}2[Al(OC(CF_3)_2CH_3)_4]^-$. (b) SQUID magnetometry of $\mathbf{44}^{2+}2SbF_6^-$ (up) and $\mathbf{45}^{2+}2SbF_6^-$ (down). Reproduced with permission [101]. Copyright 2017, American Chemical Society. (c) SQUID magnetometry of $\mathbf{30}^{2+\cdot}2[Al(OC(CF_3)_2CH_3)_4]^-$. Reproduced with permission [102]. Copyright 2018, American Chemical Society.

$\mathbf{45}^{2+}2SbF_6^-$. At the same time, the χ_MT value of $\mathbf{44}^{2+}2SbF_6^-$ and $\mathbf{45}^{2+}2SbF_6^-$ at different temperature indicated their distinctive intramolecular ferromagnetic and intramolecular antiferromagnetic interaction, respectively. This investigation provided a new insight into the design of polyradical systems and related materials.

Soon afterwards, Wang and Rajca *et al.* reported the second example of triplet diradicals-based 1D antiferromagnetic spin-1 ($S = 1$) chains, which could provide a better understanding of the low-dimensional magnetism [102]. Diradical cation macrocycle $\mathbf{30}^{2+\cdot}2[Al(OC(CF_3)_2CH_3)_4]^-$ (Fig. 10a) was very stable and obtained in good yield. The magnetic behavior for $\mathbf{30}^{2+}$ was best modeled by 1D spin $S = 1$ Heisenberg chain from 80 K to 348 K with intrachain antiferromagnetic coupling (Fig. 10c). In addition, the packing of $\mathbf{30}^{2+\cdot}2[Al(OC(CF_3)_2CH_3)_4]^-$ was in the form of 1D chains, and the intrachain exchange coupling between the radical macrocycle was antiferromagnetic on account of interaryl C···C contacts and π-π interactions. Interestingly, a weak ferromagnetic exchange coupling originating from the negligible non-overlapped π-π interaction between chains by the $[Al(OC(CF_3)_2CH_3)_4]^-$ anions was observed in this work. This investigation provided a novel system to study the low-dimensional magnetism.

The approximate 120° angle of two phenyl in TPA moiety makes it a good building block for the construction of novel π-conjugated macrocycles. For example, Fang and Lai *et al.*, for the first time, reported the synthesis of TPA derivatized phenylacetylene macrocycle **46** (Fig. 11a) in 2012 [103]. The simulated structure of **46** indicated the macrocycle was almost plane whose cavity was approximately 19.55 Å (Fig. 11b). Subsequently, electrochemical measurement of macrocycle **46** showed two oxidation peaks at 0.410 and 0.640 V, which were related to $\mathbf{46}\rightarrow\mathbf{46}^{3+}$ and $\mathbf{46}^{3+}\rightarrow\mathbf{46}^{6+}$, respectively (Fig. 11c). This research may be in favor of synthesizing multifarious conjugated TPA radical macrocycles.

Except for phenylacetylene macrocycles, TPA moiety can also be employed in the backbone of annulene to construct annulene-like TPA macrocycle. Chi *et al.* reported a new π-conjugated macrocycle **47** (Fig. 12a) containing *para*-quinodimethane and TPA moiety, which displayed annulene-like anti-aromaticity at low temperatures due to its rigid conformation and effective π-conjugation [104]. The radical cationic species of **47**, namely $\mathbf{47}^{+}SbF_6^-$, $\mathbf{47}^{2+}2SbF_6^-$, $\mathbf{47}^{3+}3SbF_6^-$, and $\mathbf{47}^{4+}4SbF_6^-$ (Figs. 12b-e) can be generated by addition of 1–4 equiv. of $AgSbF_6$. Interestingly, $\mathbf{47}^{2+}$ and $\mathbf{47}^{4+}$ exhibited global aromaticity and antiaromaticity following the Hückel rule, respectively, as indicated by NMR measurement and theoretical calculations. Moreover, both $\mathbf{47}^{2+}$ and $\mathbf{47}^{4+}$ showed open-shell singlet ground states with small singlet-triplet gap. This research may provide new synthetic approach to construct more complicated π-conjugated macrocycles as well as three-dimensional cages, which has been realized in the recent reports [105,106].

Shimizu *et al.* synthesized TPA macrocycle **48** (Fig. 13a) for the first time to investigate the effect on the ability to generate radical after binding different guest molecules [107]. Notably, most of the TPA radical cations are generated by chemical oxidation, while irradiation is successfully employed in their work to generate radical cation. The activated macrocycle **48** showed a broad and axial powder pattern shape EPR signal under UV irradiation with

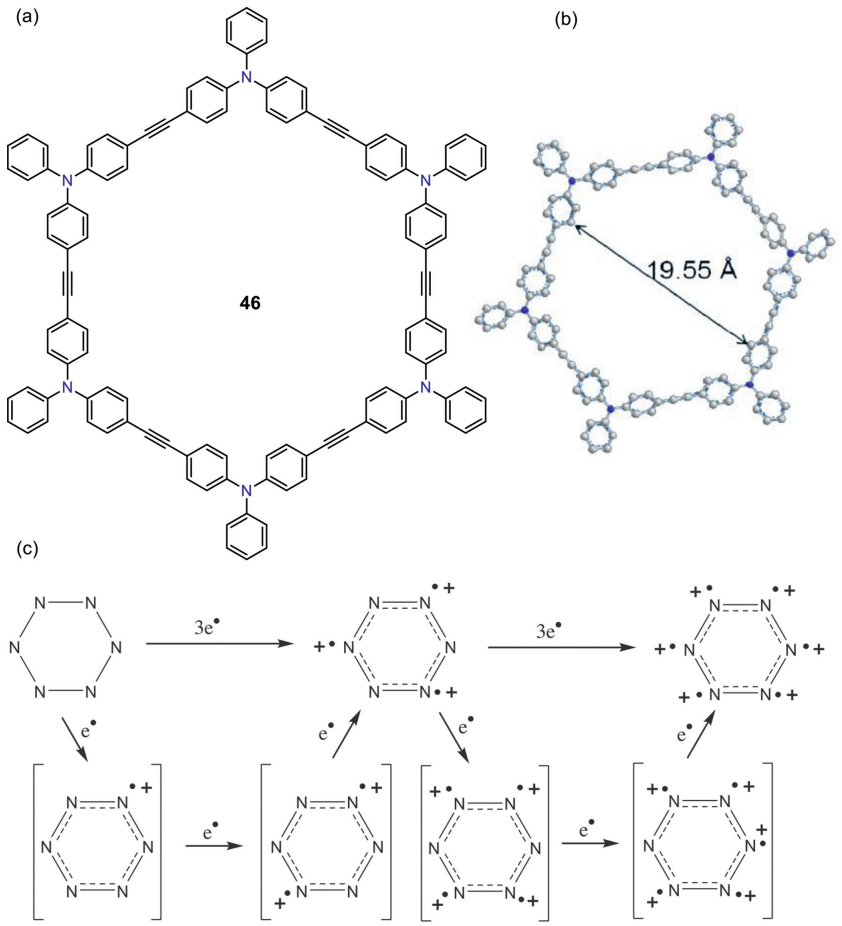

Fig. 11. (a) Chemical structure of macrocycle **46**. (b) Simulated structure of macrocycle **46**. (b) Oxidation of macrocycle **46** to $\mathbf{46}^{3+}$ and $\mathbf{46}^{6+}$. Reproduced with permission [103]. Copyright 2012, Elsevier.

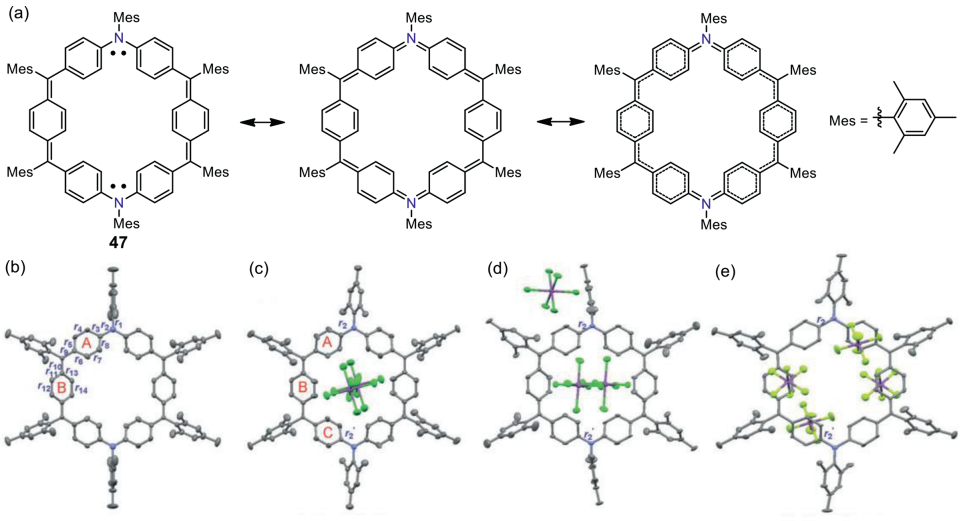

Fig. 12. (a) Several representative resonance forms of the neutral macrocycle **47**. (b-e) Single crystal structures of **47**, $\mathbf{47}^{2+}2SbF_6^-$, $\mathbf{47}^{3+}3SbF_6^-$, and $\mathbf{47}^{4+}4SbF_6^-$. Reproduced with permission [104]. Copyright 2019, John Wiley and Sons.

365 nm LEDs. Interestingly, it was found that the guest molecules with increased polarity or heavy atom substitution decreased the number of the generated radicals, while they had little influence on the absorption, emission, and photoluminescence lifetimes of macrocycle **48** in both solution and solid states. What is more, the formation/decay process of radical cation can continue over several cycles with reproducible results and occurred without degradation of the host material. The regeneration of radical proved the radical signal could be almost fully restored in both intensity and shape (Fig. 14).

Shi, Ding and Yang *et al.* designed and reported the first TPA-based metal coordination macrocycle with ability to generate radicals under irradiating [108] in spite of the difficulty to introduction organic radicals into metal coordination macrocycle. Well-defined

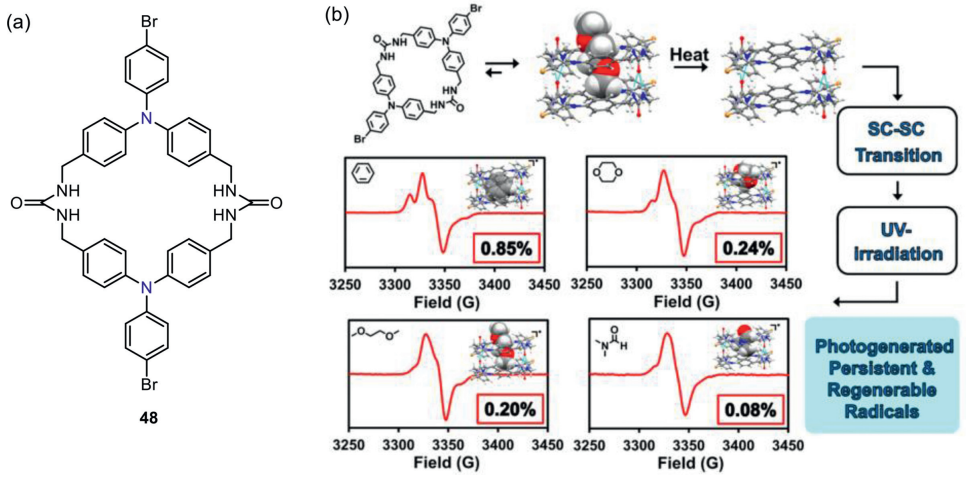

Fig. 13. (a) Chemical structure of macrocycle **48**. (b) Self-assembly of macrocycle **48** results in the formation of a columnar assembled host. Activation of this host by heating allows for the introduction of new guests *via* SC-SC transformations. Reproduced with permission [107]. Copyright 2020, American Chemical Society.

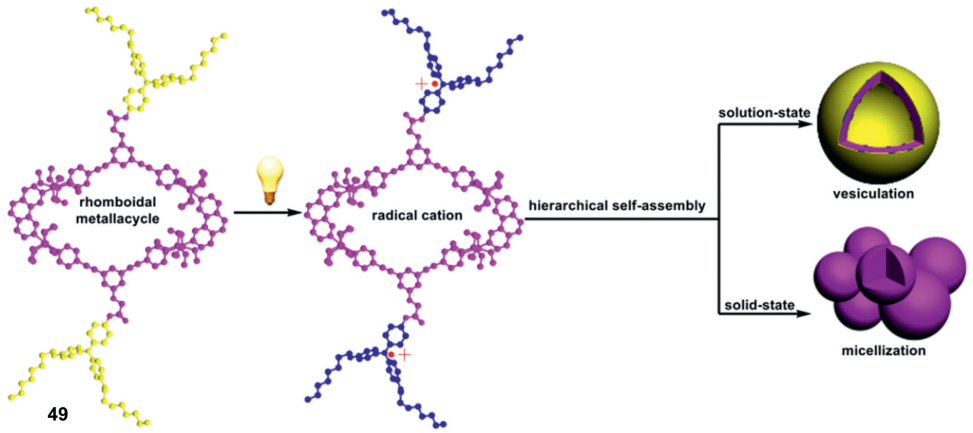

Fig. 14. Chemical structure of macrocycle **49** and self-assembly of its radical species. Reproduced with permission [108]. Copyright 2019, American Chemical Society.

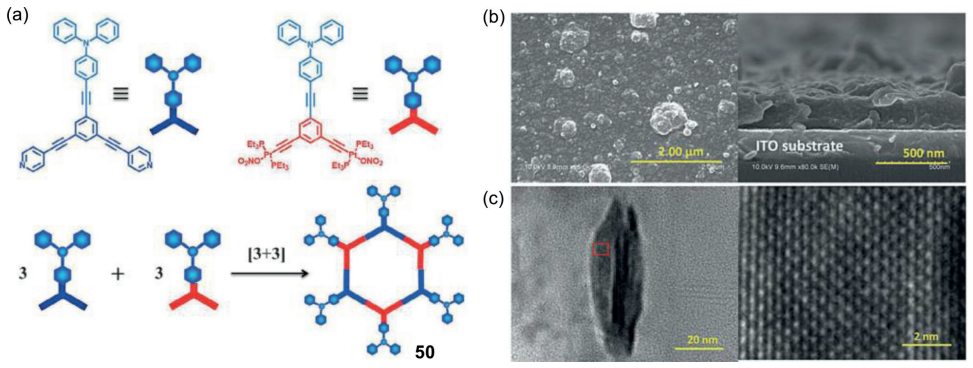

Fig. 15. (a) Graphical representation of the self-assembly of metallacycle **50**. (b) Top view (left) and side view (right) of representative SEM pictures of the porous membrane film. (c) TEM micrographs of the thin film fragment at low magnification (left) and the enlarged area (right). Reproduced with permission [109]. Copyright 2016, John Wiley and Sons.

rhomboidal metal coordination macrocycle **49** (Fig. 15) contained TPA moiety in their framework was successfully constructed by coordination-driven self-assembly approach. TPA moiety in macrocycle **49** was demonstrated to be partially generated under white light by a photo induced electron transfer process, which would drive subsequent self-assembly in both solution and solid. As a consequence, the macrocycle bearing radical cation species self-assembled into vesicle in the solution and nanospheres in the solid state, which were confirmed by TEM and high-angle annular dark-field STEM. The mechanism of the distinct morphologies formation was correlated to both TPA radical interaction as well as metallacycle stacking interaction. What is more, the stability of the generated TPA radical cation was significantly increased in these metallacycles during the hierarchical self-assembly process, thereby opening a new way to develop stable organic radical cation in the future.

Electropolymerization of TPA is known as an effective handle to synthesize donor-acceptor conjugated polymers. Zhong and Yang *et al.* synthesized metallacycle **50** bearing TPA moiety through coordination-driven self-assembly (Fig. 15a) [109]. In this

study, two phenyl rings in the TPA unit are parent without the *para*-substitution, which provides reactive sites for the oxidative polymerization. Consequently, the electropolymerization of metallacycle **50** led to the structurally defined porous membranes, which was well characterized by the SEM and TEM measurement (Figs. 15b and c). Interestingly, the cyclic voltammetry study of the porous membranes and a series of guest molecules revealed that the membranes displayed a good size selective molecular-sieving behavior. Thus, the combination of TPA radical dimerization and coordination-driven self-assembly may provide a new design methodology to construct diverse well-controlled porous materials.

4. Conclusion

In summary, this review mainly summarizes the recent development of triphenylamine radical cation including their design strategy, synthesis, and applications. A various of TPA radical macrocycles, ranging from their preparation method, redox and magnetic properties are particularly surveyed. Generally, TPA radical cations are generated by oxidation reaction, irradiation or electrochemical oxidation from their neutral TPA counterparts. To date, many TPA radical cations including their synthetic method, stability strategy have been well studied. However, the reports of TPA radical cation-based macrocycles are relatively few because the study of TPA radical cation-based macrocycles still remains a challenge. On the one hand, the efficient synthesis of TPA macrocycle, especially the fully conjugated ones, is the prerequisite to investigate their radical cationic counterparts. Thus, the rational molecular design of novel TPA-based macrocycle is very important. On the other hand, the new strategy of stabilizing TPA radical cation species within the macrocycle is highly expected. In our opinion, the future research in this field should not limit to macrocyclic system, more sophisticated architectures, *e.g.*, cages, dendrimers, interlocked complexes, bearing TPA radical cations need to be urgently exploited. Besides, more research focus should be paid to the application of TPA radical macrocycle-based advanced materials and their practical applications. We anticipate that this mini review will not only give the generalization and summary of TPA radical cations and related macrocycles but also shed new light on the prospect of the design of more sophisticated radical cation-based architectures and related materials.

Declaration of competing interest

The authors declare that no conflict of interest exits in the submission of this manuscript, and the manuscript is approved by all authors for publication.

Acknowledgments

H.-B. Yang thanks the Innovation Program of Shanghai Municipal Education Commission (No. 2019–01–07–00–05-E00012) and Program for Changjiang Scholars and Innovative Research Team in University for financial support. X. Shi acknowledges the financial supports sponsored by NSFC/China (Nos. 22071061, 52003081), Shanghai Sailing Program (No. 19YF1412900), and Microscale Magnetic Resonance Platform of ECNU.

References

[1] A.D. McNaught, A. Williamson, International Union of Pure and Applied Chemistry, Compendium of Chemical Terminology, 2nd ed., Blackwell Science, Cambridge, 1997.
[2] M. Hayyan, M.A. Hashim, I.M. AlNashef, Chem. Rev. 116 (2016) 3029–3085.
[3] G. Herzberg, The Spectra and Structures of Simple Free Radicals: An Introduction to Molecular Spectroscopy, Dover Publications, Inc., Mineola, NY, 2003.
[4] Z.V. Todres, Ion-radical Organic Chemistry: Principles and Applications, 2ed, CRC Press Taylor & Francis Group, Boca Raton, Florida, USA, 2008.
[5] R.G. Hicks, Stable Radicals: Fundamentals and Applied Aspects of Odd-Electron Compounds, Wiley, New York, 2010.
[6] D. Griller, K.U. Ingold, Acc. Chem. Res. 9 (1976) 13–19.
[7] U. Geiser, J.A. Schlueter, Chem. Rev. 104 (2004) 5203–5241.
[8] T. Nishinaga, K. Komatsu, Org. Biomol. Chem. 3 (2005) 561–569.
[9] D. Sakamaki, S. Ghosh, S. Seki, Mater. Chem. Front. 3 (2019) 2270–2282.
[10] B. Tang, J. Zhao, J.F. Xu, X. Zhang, Chem. Sci. 11 (2020) 1192–1204.
[11] M. Gomberg, J. Am. Chem. Soc. 22 (1900) 757–771.
[12] G.F. Huo, Q. Tu, X.L. Zhao, et al., Chin. Chem. Lett. 31 (2020) 1847–1850.
[13] X. Ai, E.W. Evans, S. Dong, et al., Nature 563 (2018) 536–540.
[14] H. Guo, Q. Peng, X.K. Chen, et al., Nat. Mater. 18 (2019) 977–984.
[15] Y. Wang, S. Qiu, S. Xie, et al., J. Am. Chem. Soc. 141 (2019) 2169–2176.
[16] C. Jiang, Y. Bang, X. Wang, et al., Chem. Commun. 54 (2018) 2389–2392.
[17] O. Armet, J. Veciana, C. Rovira, et al., J. Phys. Chem. 91 (1987) 5608–5616.
[18] C.F. Koelsch, J. Am. Chem. Soc. 79 (1957) 4439–4441.
[19] S.H. Jang, P. Gopalan, J.E. Jackson, B. Kahr, Angew. Chem. Int. Ed. 33 (1994) 775–777.
[20] D.H. Reid, Tetrahedron 3 (1958) 339–352.
[21] O.L. Lebedev, S.N. Kazarnovskii, Zh. Obshch. Khim. 30 (1960) 1631–1635.
[22] J. Lu, Y. Chen, X. Wen, et al., J. Phys. Chem. A 103 (1999) 6998–7007.
[23] X. Pan, X. Chen, T. Li, Y. Li, X. Wang, J. Am. Chem. Soc. 135 (2013) 3414–3417.
[24] J.E. Leffler, G.B. Watts, T. Tanigaki, et al., J. Am. Chem. Soc. 92 (1970) 6825–6830.
[25] G. Tan, X. Wang, Acc. Chem. Res. 50 (2017) 1997–2006.
[26] E. Moulin, J.J. Armao IV, N. Giuseppone, Acc. Chem. Res. 52 (2019) 975–983.
[27] J. Wang, K. Liu, L. Ma, X. Zhan, Chem. Rev. 116 (2016) 14675–14725.
[28] T.A. Schaub, T. Mekelburg, P.O. Dral, et al., Chem. Eur. J. 26 (2020) 3264–3269.
[29] M. Kuratsu, M. Kozaki, K. Okada, Angew. Chem. Int. Ed. 44 (2005) 4056–4058.
[30] X. Zheng, X. Wang, Y. Qiu, et al., J. Am. Chem. Soc. 135 (2013) 14912–14915.
[31] I. Krossing, I. Raabe, Angew. Chem. Int. Ed. 43 (2004) 2066–2090.
[32] T.A. Engesser, M.R. Lichtenthaler, M. Schleep, I. Krossing, Chem. Soc. Rev. 45 (2016) 789–899.
[33] I.M. Riddlestone, A. Kraft, J. Schaefer, I. Krossing, Angew. Chem. Int. Ed. 57 (2018) 13982–14024.
[34] A. Ito, J. Mater. Chem. C 4 (2016) 4614–4625.
[35] Q. Kong, D. Zhu, Y. Quan, et al., Chem. Mater. 19 (2007) 3309–3318.
[36] Y. Zhao, K. Jiang, W. Xu, D. Zhu, Tetrahedron 68 (2012) 9113–9118.
[37] K. Chen, H.R. Zhao, Z.K. Fan, et al., Org. Lett. 17 (2015) 1413–1416.
[38] S.Q. Zhang, Z.Y. Liu, W.F. Fu, et al., ACS Nano 11 (2017) 11701–11713.
[39] I. Saha, E.B. Wang, C.A. Parish, K. Ghosh, ChemistrySelect 2 (2017) 4794–4799.
[40] L. Vacareanu, O.I. Negru, M. Grigoras, J. Polym. Sci. A: Polym. Chem. 56 (2018) 2565–2573.
[41] L. Yuan, Y. Han, T. Tao, H. Phan, C. Chi, Angew. Chem. Int. Ed. 57 (2018) 9023–9027.
[42] B. Zhang, C. Wang, L. Wang, Y. Chen, J. Mater. Chem. C 6 (2018) 4023–4029.
[43] A.J. Sindt, M.D. Smith, S. Berens, et al., Chem. Commun. 55 (2019) 5619–5622.
[44] H. Wieland, Chem. Ber. 40 (1907) 4260–4281.
[42] M.R. Talipov, M.M. Hossain, A. Boddeda, et al., Org. Biomol. Chem. 14 (2016) 2961–2968.
[46] T. Michinobu, E. Tsuchida, H. Nishide, Bull. Chem. Soc. Jpn. 73 (2000) 1021–1027.
[47] J.A. Christensen, B.T. Phelan, S. Chaudhuri, et al., J. Am. Chem. Soc. 140 (2018) 5290–5299.
[48] S. Hiraoka, T. Okamoto, M. Kozaki, et al., J. Am. Chem. Soc. 126 (2004) 58–59.
[49] A. Ito, M. Urabe, K. Tanaka, Angew. Chem. Int. Ed. 42 (2003) 921–924.
[50] Y. Hirao, H. Ishizaki, A. Ito, et al., Eur. J. Org. Chem. 2007 (2007) 186–190.
[51] M. Shasti, S.F. Völker, S. Collavini, et al., Org. Lett. 21 (2019) 3261–3264.
[52] L. Skorka, P. Kurzep, T. Chauvire, et al., J. Phys. Chem. B 121 (2017) 4293–4298.
[53] E. Moulin, F. Niess, M. Maaloum, et al., Angew. Chem. Int. Ed. 49 (2010) 6974–6978.
[54] C. Su, F. Yang, L. Ji, et al., J. Mater. Chem. A 2 (2014) 20083–20088.
[55] J. Liu, W. Liu, E. Aydin, et al., ACS Appl. Mater. Interfaces 12 (2020) 23874–23884.
[56] P. Reinold, K. Bruchlos, S. Ludwigs, Polym. Chem. 8 (2017) 7351–7359.
[57] L. Yuan, W. Feng, K. Yamato, et al., J. Am. Chem. Soc. 126 (2004) 11120–11121.
[58] R. Jasti, J. Bhattacharjee, J.B. Neaton, C.R. Bertozzi, J. Am. Chem. Soc. 130 (2008) 17646–17647.
[59] D. Cao, Y. Kou, J. Liang, et al., Angew. Chem. Int. Ed. 48 (2009) 9721–9723.
[60] S. Dong, Y. Luo, X. Yan, et al., Angew. Chem. Int. Ed. 50 (2011) 1905–1909.
[61] W. Si, L. Chen, X.B. Hu, et al., Angew. Chem. Int. Ed. 50 (2011) 12564–12568.
[62] S. Lee, C.H. Chen, A.H. Flood, Nat. Chem. 5 (2013) 704–710.
[63] S. Sun, J.B. Shi, Y.P. Dong, et al., Chin. Chem. Lett. 24 (2013) 987–992.
[64] X. Li, B. Li, L. Chen, et al., Angew. Chem. Int. Ed. 54 (2015) 11147–11152.
[65] W. Wang, L.J. Chen, X.Q. Wang, et al., Proc. Natl. Acad. Sci. U. S. A. 112 (2015) 5597–5601.
[66] G.W. Zhang, P.F. Li, Z. Meng, et al., Angew. Chem. Int. Ed. 55 (2016) 5304–5308.
[67] S.T.J. Ryan, J.D. Barrio, R. Suardíaz, et al., Angew. Chem. Int. Ed. 55 (2016) 16096–16100.
[68] Y.C. Zhang, L. Chen, H. Wang, Chin. Chem. Lett. 27 (2016) 817–821.
[69] L. Mao, W. Pan, Y. Fu, et al., Org. Lett. 19 (2017) 18–21.
[70] G.D. Bo, G. Dolphijn, C.T. McTernan, D.A. Leigh, J. Am. Chem. Soc. 139 (2017) 8455–8457.
[71] B. Jiang, W. Wang, Y. Zhang, et al., Angew. Chem. Int. Ed. 56 (2017) 14438–14442.
[72] W.T. Li, W.J. Qu, X. Zhu, et al., Sci. China Chem. 60 (2017) 754–760.

[73] L. Liang, Y. Chen, X.M. Chen, Y. Zhang, Y. Liu, Chin. Chem. Lett. 29 (2018) 989–991.
[74] L. Shen, N. Cao, L. Tong, et al., Angew. Chem. Int. Ed. 57 (2018) 16486–16490.
[75] Q. He, N.J. Williams, J. Hyun, et al., Angew. Chem. Int. Ed. 57 (2018) 11924–11928.
[76] X.Q. Wang, W. Wang, W.J. Li, et al., Nat. Commun. 9 (2018) 3190.
[77] H.B. Liu, Q. Zhang, M.X. Wang, Angew. Chem. Int. Ed. 57 (2018) 6536–6540.
[78] H. Ke, L.P. Yang, Mo Xie, et al., Nat. Chem. 11 (2019) 470–477.
[79] X. Wu, P. Wang, P. Turner, et al., Chem 5 (2019) 1210–1222.
[80] B. Li, B. Wang, X. Huang, et al., Angew. Chem. Int. Ed. 58 (2019) 3885–3889.
[81] D. Dai, Z. Li, J. Yang, et al., J. Am. Chem. Soc. 141 (2019) 4756–4763.
[82] L. Mao, Y. Hu, Q. Tu, et al., Nat. Commun. 11 (2020) 5806.
[83] X. Sheng, E. Li, Y. Zhou, et al., J. Am. Chem. Soc. 142 (2020) 6360–6364.
[84] L. Shen, N. Cao, L. Tong, et al., Angew. Chem. Int. Ed. 57 (2018) 16486–16490.
[85] T. Jiao, K. Cai, J.N. Nelson, et al., J. Am. Chem. Soc. 141 (2019) 16915–16922.
[86] B. Li, L. Cui, C. Li, Angew. Chem. Int. Ed. 59 (2020) 22012–22016.
[87] J. Chen, Y. Zhang, Z. Meng, et al., Chem. Sci. 11 (2020) 6275–6282.
[88] O. Anamimoghadam, L.O. Jones, J.A. Cooper, et al., J. Am. Chem. Soc. 143 (2021) 163–175.
[89] Y. Ni, T.Y. Gopalakrishna, S. Wu, J. Wu, Angew. Chem. Int. Ed. 59 (2020) 7414–7418.
[90] L. Ren, T.Y. Gopalakrishna, I.H. Park, et al., Angew. Chem. Int. Ed. 59 (2020) 2230–2234.
[91] G. Li, T. Matsuno, Y. Han, et al., Angew. Chem. Int. Ed. 59 (2020) 9727–9735.
[92] M.A. Sabuj, M.M. Huda, N. Rai, iScience 23 (2020) 101675.
[93] T.D. Selby, S.C. Blackstock, Org. Lett. 1 (1999) 2053–2055.
[94] S.I. Hauck, K.V. Lakshmi, J.F. Hartwig, Org. Lett. 1 (1999) 2057–2060.
[95] Akihiro Ito, Syuuzi Inoue, Yasukazu Hirao, et al., Chem. Commun. (2008) 3242–3244.
[96] D. Sakamaki, A. Ito, K. Furukawa, T. Kato, K. Tanaka, J. Org. Chem. 78 (2013) 2947–2956.
[97] I. Kulszewicz-Bajer, V. Maurel, S. Gambarelli, et al., Phys. Chem. Chem. Phys. 11 (2009) 1362–1368.
[98] A. Ito, Y. Yokoyama, R. Aihara, et al., Angew. Chem. Int. Ed. 49 (2010) 8205–8208.
[99] T.F. Yang, K.Y. Chiu, H.C. Cheng, et al., J. Org. Chem. 77 (2012) 8627–8633.
[100] D. Sakamaki, A. Ito, Y. Tsutsui, S. Seki, J. Org. Chem. 82 (2017) 13348–13358.
[101] R. Kurata, D. Sakamaki, A. Ito, Org. Lett. 19 (2017) 3115–3118.
[102] W. Wang, C. Chen, C. Shu, et al., J. Am. Chem. Soc. 140 (2018) 7820–7826.
[103] Z. Fang, M. Samoc, R.D. Webster, A. Samoc, Y.H. Lai, Tetrahedron Lett. 53 (2012) 4885–4888.
[104] S. Dong, T.Y. Gopalakrishna, Y. Han, C. Chi, Angew. Chem. Int. Ed. 58 (2019) 11742–11746.
[105] Y. Ni, T.Y. Gopalakrishna, H. Phan, et al., Nat. Chem. 12 (2020) 242–248.
[106] Y. Ni, F. Gordillo-Gámez, M.P. Alvarez, et al., J. Am. Chem. Soc. 142 (2020) 12730–12742.
[107] A.J. Sindt, B.A. DeHaven, D.W. Goodlett, et al., J. Am. Chem. Soc. 142 (2020) 502–511.
[108] G.F. Huo, X. Shi, Q. Tu, et al., J. Am. Chem. Soc. 141 (2019) 16014–16023.
[109] X.D. Xu, C.J. Yao, L.J. Chen, et al., Chem. Eur. J. 22 (2016) 5211–5218.